DALTON

Synthesis, solution and magic angle spinning tin-119 nuclear magnetic resonance studies and crystal structures of dithioether complexes of tin(IV) halides

Sandra E. Dann, Anthony R. J. Genge, William Levason and Gillian Reid

Department of Chemistry, University of Southampton, Highfield, Southampton SO17 1BJ, UK

The compounds SnX_4 reacted with 1 molar equivalent of dithioether, L–L, in dry $CHCl_3$ solution to give the six-co-ordinate species $[SnX_4(L{-}L)]$ [X = Cl, L–L = $MeS(CH_2)_nSMe$, o-$C_6H_4(SMe)_2$ or $PhS(CH_2)_nSPh$ (n = 2 or 3); X = Br, L–L = $MeS(CH_2)_nSMe$ or o-$C_6H_4(SMe)_2$] in high yield as white or pale yellow powdered solids. Using $SnBr_4$ and $PhS(CH_2)_nSPh$ or SnI_4 with $MeS(CH_2)_nSMe$ did not produce isolable products, although solution ^{119}Sn-$\{^1H\}$ NMR spectroscopy provided evidence for their existence at low temperatures. X-Ray structural studies on $[SnCl_4\{MeS(CH_2)_2SMe\}]$, $[SnCl_4\{MeS(CH_2)_3SMe\}]$, $[SnCl_4\{o\text{-}C_6H_4(SMe)_2\}]$, $[SnCl_4\{PhS(CH_2)_3SPh\}]$ and $[SnBr_4\{MeS(CH_2)_3SMe\}]$ confirmed an S_2X_4 donor set with the dithioether acting as a bidentate chelate. Variable-temperature solution ^1H and ^{119}Sn-$\{^1H\}$ NMR spectroscopic studies showed that the complexes are extremely labile and ligand dissociation and pyramidal inversion are fast except at low temperatures. Magic angle spinning ^{119}Sn NMR data for $[SnCl_4(L{-}L)]$ are reported. The crystal structure of *cis*-$[SnI_4\{MeS(O)(CH_2)_3SMe\}_2]$, obtained as a decomposition product from the SnI_4–$MeS(CH_2)_3SMe$ reaction, shows monodentate sulfoxide (O) co-ordination.

The co-ordination chemistry of the p-block metals has attracted much less effort than that of the transition metals. In the case of tin(IV) halides, complexes with O and N donors have long been known [1,2] and there has been some recent interest in phosphine complexes.[3] Studies with neutral sulfur-donor ligands are very limited.[4–8] The complexes *cis*- and *trans*-$[SnCl_4(Me_2S)_2]$ have been studied in detail by Merbach and co-workers,[4,5] and the reaction of Me_2SBr_2 with tin powder has been shown [7] to yield both isomers of $[SnBr_4(Me_2S)_2]$ which were structurally characterised. The structure of one tridentate thioether complex $[Sn([9]aneS_3)Cl_3][SbCl_6]$ ([9]aneS$_3$ = 1,4,7-trithiacyclononane) has also been reported.[8] Here we report the results of a systematic study of complexes of a range of dithioethers with $SnCl_4$, $SnBr_4$ and SnI_4, with particular emphasis on the characterisation by multinuclear NMR methods [in solution by ^1H and ^{119}Sn-$\{^1H\}$ and solid-state magic angle spinning (MAS) ^{119}Sn] and X-ray crystallography.

Results and Discussion

Reaction of SnX_4 with 1 molar equivalent of dithioether, L–L, in dry $CHCl_3$ solution gives the six-co-ordinate species $[SnX_4(L{-}L)]$ [X = Cl, L–L = $MeS(CH_2)_2SMe$, $MeS(CH_2)_3SMe$, o-$C_6H_4(SMe)_2$, $PhS(CH_2)_2SPh$ or $PhS(CH_2)_3SPh$; X = Br, L–L = $MeS(CH_2)_2SMe$, $MeS(CH_2)_3SMe$ or o-$C_6H_4(SMe)_2$] in high yield as white or pale yellow powdered solids. Similar reactions using $SnBr_4$ with $PhS(CH_2)_2SPh$ or $PhS(CH_2)_3SPh$ or using SnI_4 with L–L did not lead to isolable products, although in certain cases the tin(IV) dithioether adducts were observed *in situ* using ^{119}Sn-$\{^1H\}$ NMR spectroscopy (see below). Treatment of SnF_4 with L–L in refluxing CH_2Cl_2 or tetrahydrofuran (thf) solution gave no identifiable tin fluoride–dithioether adducts. Examples of co-ordination complexes of tin fluoride are largely limited to derivatives of oxygen- and nitrogen-donor ligands.[1]

The solid complexes are hydrolysed only slowly in air, but are more sensitive to moisture in solution, and the use of dry solvents is essential for spectroscopic studies. The IR spectra showed the presence of the ligand and had several strong vibrations (Experimental section) assignable as $\nu(SnX_4)$ (theory $2A_1 + B_1 + B_2$), and confirmed the absence of water or sulfoxide groups. Attempts to observe molecular ions in the mass spectra either by electrospray or FAB techniques were not successful.

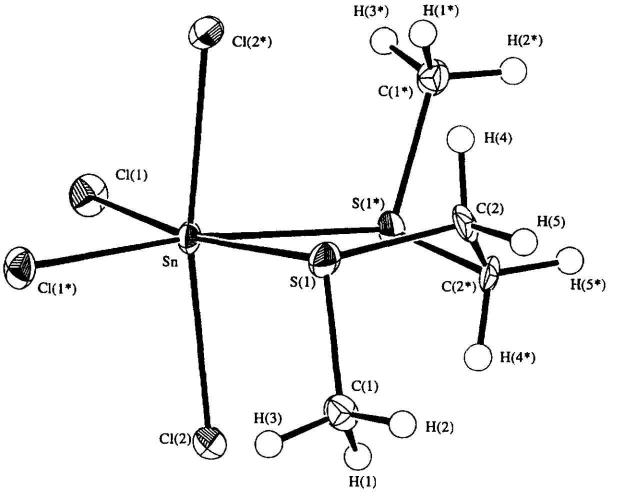

Fig. 1 View of the structure of $[SnCl_4\{MeS(CH_2)_2SMe\}]$ with the numbering scheme adopted. Ellipsoids are shown at 40% probability and atoms marked with an asterisk are related by a crystallographic two-fold axis at ($\frac{1}{2}$, 0, z)

In view of the lack of well characterised examples of dithioether complexes of Sn^{IV} and in an attempt to identify trends in their geometric parameters, and to correlate these with their behaviour in solution (by variable-temperature ^{119}Sn-$\{^1H\}$ and ^1H NMR spectroscopy), we undertook single-crystal X-ray structure analyses on several of the products. Suitable crystals were obtained either by cooling solutions of the compounds in $CHCl_3$ or by slow evaporation from solutions in acetone.

The structure of $[SnCl_4\{MeS(CH_2)_2SMe\}]$ (Fig. 1, Table 1) shows the Sn^{IV} occupying a crystallographic two-fold axis ($\frac{1}{2}$, 0, z), giving a distorted-octahedral arrangement of four Cl atoms

Table 1 Selected bond lengths (Å) and angles (°) for $[SnCl_4\{MeS(CH_2)_2SMe\}]$

Sn–Cl(1)	2.372(4)	S(1)–C(1)	1.80(1)
Sn–Cl(2)	2.413(3)	S(1)–C(2)	1.80(1)
Sn–S(1)	2.619(4)	C(2)–C(2*)	1.51(3)
Cl(1)–Sn–Cl(1*)	98.2(2)	Cl(1)–Sn–Cl(2*)	93.4(1)
Cl(1)–Sn–Cl(2)	93.2(1)	Cl(1)–Sn–S(1)	171.1(1)
Cl(1)–Sn–S(1*)	89.04(10)	Cl(2)–Sn–Cl(2*)	169.9(2)
S(1)–Sn–S(1*)	84.2(2)	Cl(2)–Sn–S(1)	81.2(1)
Sn–S(1)–C(2)	99.4(4)	Cl(2)–Sn–S(1*)	91.3(1)
S(1)–C(2)–C(2*)	116.1(7)	Sn–S(1)–C(1)	108.9(4)
		C(1)–S(1)–C(2)	102.1(6)

Table 2 Selected bond lengths (Å) and angles (°) for $[SnCl_4\{MeS(CH_2)_3SMe\}]$

Sn–Cl(1)	2.378(2)	S(1)–C(1)	1.799(7)
Sn–Cl(2)	2.409(2)	S(1)–C(2)	1.821(6)
Sn–S(1)	2.667(2)	C(2)–C(3)	1.526(8)
Cl(1)–Sn–Cl(1*)	96.32(8)	Cl(1)–Sn–Cl(2)	94.94(6)
Cl(1)–Sn–Cl(2*)	90.37(6)	Cl(1)–Sn–S(1)	172.24(6)
Cl(1)–Sn–S(1*)	90.16(5)	Cl(2)–Sn–Cl(2*)	172.04(8)
Cl(2)–Sn–S(1*)	89.27(6)	Cl(2)–Sn–S(1)	84.80(6)
S(1)–Sn–S(1*)	83.73(7)	Sn–S(1)–C(1)	105.1(2)
Sn–S(1)–C(2)	102.1(2)	C(1)–S(1)–C(2)	99.6(3)
S(1)–C(2)–C(3)	111.2(4)	C(2)–C(3)–C(2*)	115.3(7)

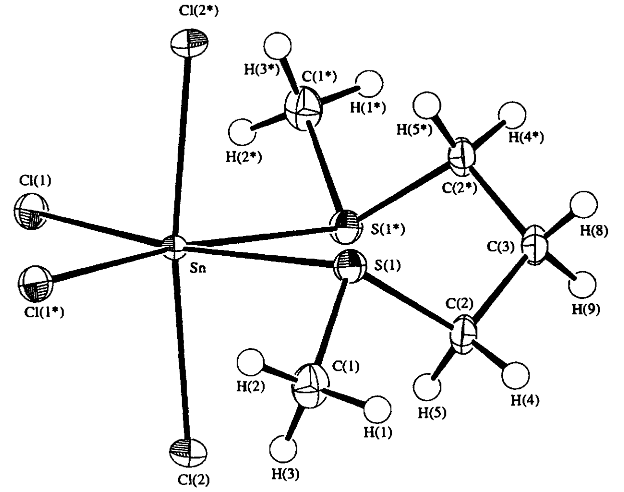

Fig. 2 View of the structure of $[SnCl_4\{MeS(CH_2)_3SMe\}]$ with the numbering scheme adopted. Ellipsoids are shown at 40% probability and atoms marked by an asterisk are related by a crystallographic two-fold axis at (1, 0, *z*)

and one chelating $MeS(CH_2)_2SMe$ ligand, Sn–S(1) 2.619(4) Å. The Sn–Cl(1) bond length [2.372(4) Å] (Cl *trans* to S) is significantly shorter than Sn–Cl(2) [2.413(3) Å] (Cl *trans* to Cl), presumably reflecting the greater *trans* influence of Cl over S (thioether). The angle at Sn involving the five-membered chelate ring [S(1)–Sn–S(1*)] is 84.2(2)°, while the other angles at Sn involving mutually *cis* donor atoms lie in the range 81.2(1)–93.4(1)°. The co-ordinated dithioether is in the DL configuration. The species $[SnCl_4\{MeS(CH_2)_3SMe\}]$ (Fig. 2, Table 2) and $[SnBr_4\{MeS(CH_2)_3SMe\}]$ (Fig. 3, Table 3) are isostructural, with the Sn atom occupying a crystallographic two-fold axis (1, 0, *z*) in each, co-ordinated to four halogen atoms and a chelating dithioether giving a distorted-octahedral geometry, with the ligand adopting the DL configuration. The bond-length trends parallel those for $[SnCl_4\{MeS(CH_2)_2SMe\}]$ described above, with Sn–X *trans* to X [X = Cl, 2.409(2); X = Br, 2.562(3) Å] being significantly longer than Sn–X *trans* to S [X = Cl, 2.378(2); X = Br, 2.533(3) Å]. The Sn–S bond lengths are 2.667(2) and 2.700(7) Å for X = Cl and Br respectively, indicating a slight lengthening in the bromo compared to the chloro species.

Table 3 Selected bond lengths (Å) and angles (°) for $[SnBr_4\{MeS(CH_2)_3SMe\}]$

Sn–Br(1)	2.533(3)	S(1)–C(1)	1.81(2)
Sn–Br(2)	2.562(3)	S(1)–C(3)	1.80(3)
Sn–S(1)	2.700(7)	C(1)–C(2)	1.51(3)
Br(1)–Sn–Br(1*)	95.9(1)	Br(1)–Sn–Br(2)	94.71(9)
Br(1)–Sn–Br(2*)	90.46(9)	Br(1)–Sn–S(1)	91.0(2)
Br(1)–Sn–S(1*)	171.7(2)	Br(2)–Sn–Br(2*)	172.3(1)
Br(2)–Sn–S(1)	84.3(2)	Br(2)–Sn–S(1*)	89.9(2)
S(1)–Sn–S(1*)	82.5(3)	Sn–S(1)–C(1)	102.5(9)
Sn–S(1)–C(3)	105.0(8)	C(1)–S(1)–C(3)	99(1)
S(1)–C(1)–C(2)	111(1)	C(1)–C(2)–C(1*)	116(2)

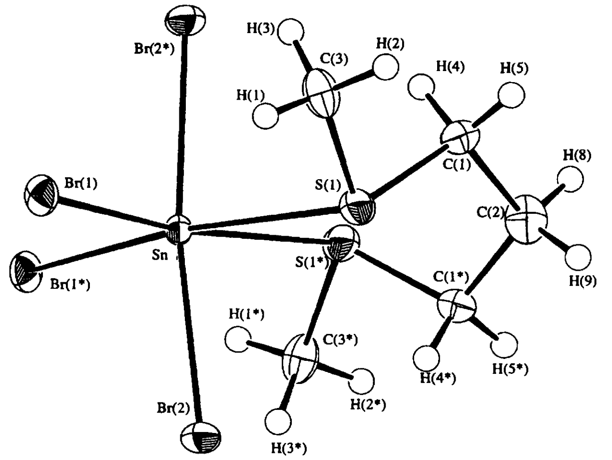

Fig. 3 View of the structure of $[SnBr_4\{MeS(CH_2)_3SMe\}]$ with the numbering scheme adopted. Details as in Fig. 2

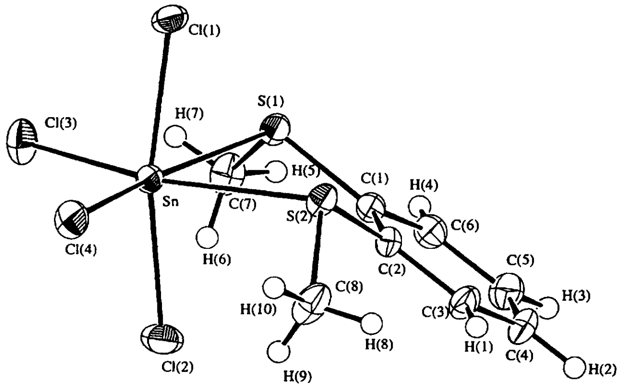

Fig. 4 View of the structure of $[SnCl_4\{o\text{-}C_6H_4(SMe)_2\}]$ with the numbering scheme adopted. Ellipsoids are shown at 40% probability

The structure of $[SnCl_4\{o\text{-}C_6H_4(SMe)_2\}]$ shows (Fig. 4, Table 4) the molecule occupying a general position. Again the Sn atom is ligated to four Cl atoms and a chelating dithioether, however in this case the dithioether adopts the *meso* configuration, Sn–Cl(1) 2.401(2), Sn–Cl(2) 2.383(2) (Cl *trans* to Cl), Sn–Cl(3) 2.357(2), Sn–Cl(4) 2.357(2) (Cl *trans* to S), Sn–S(1) 2.659(2) and Sn–S(2) 2.677(2) Å. The complex $[SnCl_4\{PhS(CH_2)_3SPh\}]$ (Fig. 5, Table 5) adopts a similar distorted-octahedral structure, with the chelating ligand in the DL configuration. Notably, the Sn–S distances [2.724(5), 2.725(5) Å] are significantly longer than in any of the other

Table 4 Selected bond lengths (Å) and angles (°) for $[SnCl_4\{o\text{-}C_6H_4(SMe)_2\}]$

Sn–Cl(1)	2.401(2)	Sn–Cl(2)	2.383(2)
Sn–Cl(3)	2.357(2)	Sn–Cl(4)	2.357(2)
Sn–S(1)	2.659(2)	Sn–S(2)	2.677(2)
S(1)–C(1)	1.777(7)	S(1)–C(7)	1.809(8)
S(2)–C(2)	1.778(7)	S(2)–C(8)	1.809(7)
C(1)–C(2)	1.398(9)	C(1)–C(6)	1.395(9)
C(2)–C(3)	1.401(9)	C(3)–C(4)	1.38(1)
C(5)–C(6)	1.39(1)	C(4)–C(5)	1.38(1)
Cl(1)–Sn–Cl(2)	169.00(7)	Cl(1)–Sn–Cl(3)	93.14(7)
Cl(1)–Sn–Cl(4)	91.79(7)	Cl(1)–Sn–S(1)	83.28(6)
Cl(1)–Sn–S(2)	83.17(6)	Cl(2)–Sn–Cl(3)	95.57(8)
Cl(2)–Sn–Cl(4)	92.83(7)	Cl(2)–Sn–S(1)	89.87(6)
Cl(2)–Sn–S(2)	86.70(7)	Cl(3)–Sn–Cl(4)	102.73(7)
Cl(3)–Sn–S(1)	90.95(6)	Cl(3)–Sn–S(2)	165.01(6)
Cl(4)–Sn–S(1)	165.72(7)	Cl(4)–Sn–S(2)	91.93(6)
S(1)–Sn–S(2)	74.21(6)	Sn–S(1)–C(1)	102.3(2)
Sn–S(1)–C(7)	105.8(3)	C(1)–S(1)–C(7)	102.1(3)
Sn–S(2)–C(2)	100.9(2)	Sn–S(2)–C(8)	105.1(3)
C(2)–S(2)–C(8)	102.8(3)	S(1)–C(1)–C(2)	121.0(5)
S(1)–C(1)–C(6)	118.9(5)	C(2)–C(1)–C(6)	120.1(6)
S(2)–C(2)–C(1)	120.5(5)	S(2)–C(2)–C(3)	119.9(6)
C(1)–C(2)–C(3)	119.4(7)	C(2)–C(3)–C(4)	119.7(7)
C(3)–C(4)–C(5)	120.9(7)	C(4)–C(5)–C(6)	120.2(7)
C(1)–C(6)–C(5)	119.7(7)		

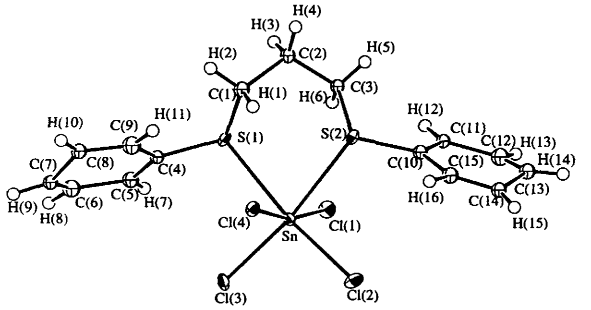

Fig. 5 View of the structure of $[SnCl_4\{PhS(CH_2)_3SPh\}]$ with the numbering scheme adopted. Ellipsoids are shown at 40% probability

Table 5 Selected bond lengths (Å) and angles (°) for $[SnCl_4\{PhS(CH_2)_3SPh\}]$

Sn–Cl(1)	2.385(5)	Sn–Cl(2)	2.379(6)
Sn–Cl(3)	2.380(5)	Sn–Cl(4)	2.376(4)
Sn–S(1)	2.724(5)	Sn–S(2)	2.725(5)
S(1)–C(1)	1.86(1)	S(1)–C(4)	1.77(1)
S(2)–C(3)	1.78(1)	S(2)–C(10)	1.80(1)
C(1)–C(2)	1.58(2)	C(2)–C(3)	1.49(2)
Cl(1)–Sn–Cl(2)	94.1(2)	Cl(1)–Sn–Cl(3)	94.6(2)
Cl(1)–Sn–Cl(4)	167.69(5)	Cl(1)–Sn–S(1)	84.0(2)
Cl(1)–Sn–S(2)	86.7(2)	Cl(2)–Sn–Cl(3)	96.55(5)
Cl(2)–Sn–Cl(4)	93.2(2)	Cl(2)–Sn–S(1)	172.7(2)
Cl(2)–Sn–S(2)	91.2(2)	Cl(3)–Sn–Cl(4)	94.4(2)
Cl(3)–Sn–S(1)	90.6(2)	Cl(3)–Sn–S(2)	172.0(2)
Cl(4)–Sn–S(1)	87.5(2)	Cl(4)–Sn–S(2)	83.3(2)
S(1)–Sn–S(2)	81.67(4)	Sn–S(1)–C(1)	99.5(4)
Sn–S(1)–C(4)	108.7(4)	C(1)–S(1)–C(4)	106.3(6)
Sn–S(2)–C(3)	103.8(4)	Sn–S(2)–C(10)	108.9(4)
C(3)–S(2)–C(10)	101.8(5)	S(1)–C(1)–C(2)	103.3(8)
S(1)–C(4)–C(9)	120.7(9)	S(1)–C(4)–C(5)	117.4(8)
S(2)–C(3)–C(2)	116.5(8)	C(1)–C(2)–C(3)	113.6(5)
S(2)–C(10)–C(11)	125.2(9)	S(2)–C(10)–C(15)	114.0(8)

structures, indicating that the Ph-substituted dithioether is a poorer ligand for Sn^{IV} than are the Me-substituted derivatives. Also, there is little difference between the Sn–Cl *trans* to Cl [2.385(5), 2.376(4) Å] and *trans* to S [2.379(6), 2.380(5) Å] bond distances in this particular species.

The Sn–S and Sn–X distances determined from this study are in good agreement with the few structurally characterised literature examples, *e.g.* $[SnCl_3([9]aneS_3)]^+$ [Sn–S 2.618(3), 2.636(3), 2.657(4), Sn–Cl 2.366(4), 2.369(3), 2.371(4) Å],[8] *cis*-$[SnBr_4(SMe_2)_2]$ [Sn–S 2.692(9), 2.692(8), Sn–Br 2.554(4), 2.532(4), 2.557(4), 2.539(4) Å][7] and *trans*-$[SnCl_4(\eta'\text{-}C_6H_{12}S_2\text{-}1,5)_2]$ ($C_6H_{12}S_2$-1,5 = 1,5-dithiacyclooctane) [Sn–S 2.602(1), Sn–Cl 2.414(1), 2.428(1) Å].[9] However, our studies also reveal some particular trends in the observed bond distances: the Sn–S bond lengths for the $SnCl_4$ adducts of the Me-substituted dithioethers $MeS(CH_2)_2SMe$, $MeS(CH_2)_3SMe$ and *o*-$C_6H_4(SMe)_2$ are shorter than for $[SnBr_4\{MeS(CH_2)_3SMe\}]$, and the Sn–S bond lengths in the Ph-substituted derivative, $[SnCl_4\{PhS(CH_2)_3SPh\}]$, are even longer. There is a close parallel between these trends in bond lengths and the observed stabilities of the various SnX_4 (X = Cl, Br or I) dithioether adducts in solution observed by $^{119}Sn\text{-}\{^1H\}$ and ^1H NMR spectroscopy as shown below.

For complexes of type $[SnX_4(L\text{–}L)]$, where L–L is a chelating dithioether ligand, two diastereoisomers (invertomers) are expected, *meso* and DL forms, which interconvert *via* pyramidal inversion at the sulfur atoms. Providing pyramidal inversion and ligand dissociation are slow on the NMR time-scale, such diastereoisomers are readily distinguishable by ^1H NMR techniques.[10] At 170 K CD_2Cl_2 solutions of $[SnCl_4\{MeS(CH_2)_nSMe\}]$ (*n* = 2 or 3) show two δ(Me) resonances (Table 6) with weak $^3J(^{119/117}Sn\text{–}^1H)$ satellites in the range 30–50 Hz. On gentle warming (> *ca.* 200 K) the lines broaden, coalesce, and then the resulting singlets sharpen on further warming. The tin satellites are also lost during this time, suggesting that the ligand-dissociation and pyramidal-inversion rates become significant at similar temperatures. The behaviour of $[SnCl_4\{o\text{-}C_6H_4(SMe)_2\}]$ is similar, although, in contrast to the dithiaalkane complexes, for the *o*-phenylene ligand complex the invertomer ratio is very disparate (*ca.* 1 : 10). The presence of invertomers in $[SnCl_4\{PhS(CH_2)_2SPh\}]$ is shown by second-order $\delta(CH_2)$ resonances at 180 K, but for $[SnCl_4\{PhS(CH_2)_3SPh\}]$ even at the lowest temperature achieved (175 K) the $\delta(CH_2)$ resonances were still broad, indicating the low-temperature-limiting spectrum had not been reached. Invertomers were identified in the ^1H NMR spectra of $[SnBr_4\{MeS(CH_2)_nSMe\}]$ at 180 K, but the spectrum of $[SnBr_4\{o\text{-}C_6H_4(SMe)_2\}]$ at 180 K showed only a single, broad δ(Me) signal with no tin satellites. Although the data are limited and the ligand dissociation occurring at similar energies precludes more detailed measurements,[6] qualitatively it is clear that inversion barriers in these tin(IV) complexes decrease with ligand substituents Me > Ph, $(CH_2)_2$ > *o*-C_6H_4, and with the *trans* ligand Cl > Br; the same trends as observed with many d-block metal complexes.

The dithiahexane complexes were poorly soluble in CH_2Cl_2, requiring long accumulations for $^{119}Sn\text{-}\{^1H\}$ NMR studies, but the other compounds were considerably more soluble. A range of other solvents was also examined including $MeNO_2$, Me_2CO, thf and propane-1,3-diol carbonate, but these proved unsatisfactory and there was a possibility that the observed resonances were due to O-donor adducts.[11]

The $^{119}Sn\text{-}\{^1H\}$ NMR spectra confirm the conclusions of the ^1H studies that these systems are very labile, and that pyramidal inversion is rapid except at low temperatures. For example $[SnCl_4\{MeS(CH_2)_3SMe\}]$ shows a broad tin resonance at 300 K (δ −567), which sharpens on cooling and below *ca.* 220 K shows two closely spaced resonances attributable to the *meso* and DL invertomers. The behaviour of $[SnCl_4\{MeS(CH_2)_2SMe\}]$ was similar, but $[SnCl_4\{o\text{-}C_6H_4(SMe)_2\}]$ showed no tin resonance at 300 K, attributed to ligand dissociation, and the $^{119}Sn\text{-}\{^1H\}$ resonance was only seen below 240 K. Ligand dissociation was greater in $[SnCl_4\{PhS(CH_2)_nSPh\}]$ and $[SnBr_4\{MeS(CH_2)_nSMe\}]$ in that tin resonances were only observable at < *ca.* 230 K, and separate resonances for the

Table 6 Proton and ^{119}Sn-{^{1}H} NMR spectroscopic data

	^{1}H (δ)[a]		^{119}Sn-{^{1}H} (δ)[b]		
Complex	300 K	175 K	300 K	180 K	^{119}Sn (δ)[c]
$[SnCl_4(Me_2S)_2]$	—	—	−572, −578	−561, −572 (2:1)	−627
$[SnCl_4\{MeS(CH_2)_2SMe\}]$	2.50	2.48, 2.61 (2:1)	−560 (br)	−548.5, −549.0	−630
$[SnCl_4\{MeS(CH_2)_3SMe\}]$	2.37	2.48, 2.64 (1:2)	−567 (br)	−558.0, −563.0	−654
$[SnCl_4\{o\text{-}C_6H_4(SMe)_2\}]$	2.75	2.80, 3.05 (1:10)	n.o.[d]	−504.2, −504.9 (sh)	−617
$[SnCl_4\{PhS(CH_2)_2SPh\}]$			n.o.	−515.0, −516.2	−618
$[SnCl_4\{PhS(CH_2)_3SPh\}]$			n.o.	−570.3	−653
$[SnBr_4(Me_2S)_2]$	—	—	n.o.	−1174, −1222 (1:1)	
$[SnBr_4(MeS(CH_2)_2SMe)]$	2.24	2.26, 2.41 (1:1)	n.o.	−1123.2, −1124.0	
$[SnBr_4(MeS(CH_2)_3SMe)]$	2.18	2.05, 2.41 (3:1)	n.o.	−1179, −1180 (br)	
$[SnBr_4\{o\text{-}C_6H_4(SMe)_2\}]$	2.50	2.86	n.o.	n.o.	

[a] In CD_2Cl_2, Me resonances only, approximate ratios in parentheses. [b] Relative to external $SnMe_4$ in CH_2Cl_2–CD_2Cl_2. [c] Magic angle spinning data from powdered solid at 300 K. [d] n.o. = No resonance observed.

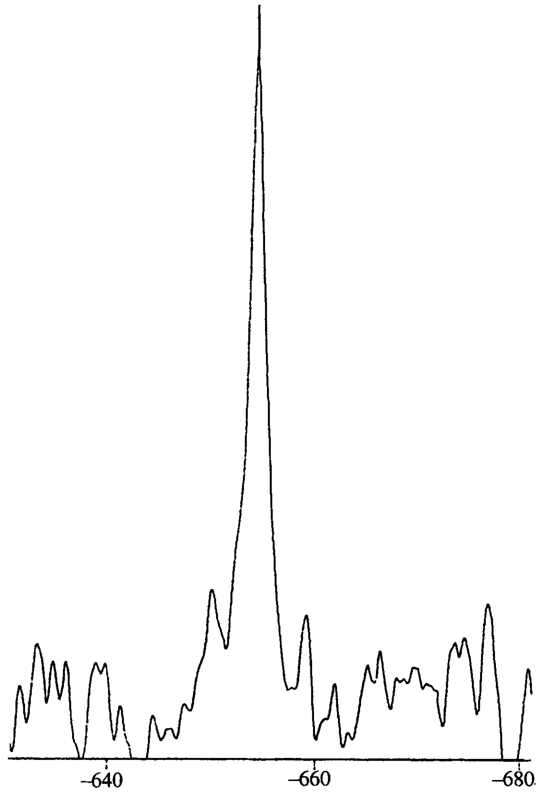

Fig. 6 The MAS ^{119}Sn NMR spectrum of $[SnCl_4\{MeS(CH_2)_3SMe\}]$ recorded at 4.5 kHz

invertomers were not seen in the case of $[SnCl_4\{PhS(CH_2)_3SPh\}]$ even at 175 K. The extreme case was $[SnBr_4\{o\text{-}C_6H_4(SMe)_2\}]$ where a tin resonance was not observed at all in the temperature range 180–300 K. No solid complexes could be isolated from $SnBr_4$ + $PhS(CH_2)_nSPh$ systems, but we observed a broad ^{119}Sn-{^{1}H} resonance at δ −1127 from solutions of $SnBr_4$ and excess of $PhS(CH_2)_2SPh$, indicative of the formation of a complex at low temperatures. Although we were unable to isolate dithioether complexes of SnI_4, the latter dissolves readily in CH_2Cl_2 in the presence of an excess of $MeS(CH_2)_nSMe$ (n = 2 or 3). At 180 K both mixtures gave broad ^{119}Sn-{^{1}H} resonances at δ −2645 (n = 3) or −2725 (n = 2) which we interpret as due to the formation of SnI_4S_2 species at low temperatures (for comparison SnI_4 in CS_2 has δ −1701).[12] Both resonances were lost on warming above 190 K.

The ^{119}Sn-{^{1}H} NMR spectra of Me_2S complexes were also examined. The $[SnCl_4(Me_2S)_2]$–Me_2S system has been studied in considerable detail by Knight and Merbach.[5] At room temperature in CH_2Cl_2 solution $[SnCl_4(Me_2S)_2]$ exhibits two resonances at δ −572 and −578 attributable to the *cis* and *trans* isomers respectively. In the presence of an excess of Me_2S the processes occurring are (in order of decreasing rate) Me_2S exchange with the *cis* isomer, *cis–trans* isomerisation, and Me_2S exchange with the *trans* isomer.[5] The complex $[SnBr_4(Me_2S)_2]$ in CH_2Cl_2 showed no tin resonance at room temperature, but a broad single resonance appeared on cooling to *ca.* 280 K. This broadened further on cooling and split into two below *ca.* 240 K, and at 180 K sharp resonances were present of approximately equal intensity at δ −1174 and −1222, assignable to the *cis* and *trans* forms. As with the bidentate complexes, the $SnBr_4$ complexes of Me_2S show greater ligand dissociation than do the chloride analogues, with increasing temperatures. A CH_2Cl_2 solution of $[SnBr_4(Me_2S)_2]$ containing an excess of Me_2S at 180 K has sharp resonances at δ −1179 and −1228. On warming to *ca.* 230 K the higher-frequency resonance due to the *cis* isomer broadens and then on further heating sharpens. At *ca.* 250 K the resonance of the *trans* isomer broadens, but even at 300 K separate resonances for both geometric isomers are still present. In contrast, we were unable to observe a ^{119}Sn-{^{1}H} resonance from solutions of SnI_4 in CH_2Cl_2 containing an excess of Me_2S at any temperature in the range 300–180 K. A solution of $SnCl_4$ in CH_2Cl_2 containing an excess of Ph_2S had a broad ^{119}Sn-{^{1}H} resonance at 190 K with δ −599, but on warming this broadened rapidly and disappeared above *ca.* 200 K. No resonances were observed from the corresponding $SnBr_4$–Ph_2S–CH_2Cl_2 systems even at 190 K. Tin(IV) fluoride did not dissolve in CH_2Cl_2 in the presence of a large excess of Me_2S.

The MAS ^{119}Sn NMR data are given in Table 6 together with the solution data collected in dichloromethane. Of note is the small chemical shift range observed for the various $SnCl_4$–dithioether species (40 ppm) in the solid state, and these are shifted by up to 100 ppm from the observed solution resonances. In all cases a singlet was observed. The resonance broadens with the lowering in symmetry in the molecular crystal structure, *e.g.* $[SnCl_4\{MeS(CH_2)_3SMe\}]$ [tetragonal space group, C_2 local symmetry at tin, δ −654, full width at half maximum (f.w.h.m.) 3 ppm] (Fig. 6) and $[SnCl_4\{o\text{-}C_6H_4(SMe)_2\}]$ (triclinic space group, C_1 local symmetry at tin, δ −617, f.w.h.m. 40 ppm). In addition to the signal broadening on lowering of the symmetry, additional spinning side bands appeared which did not collapse even at the highest possible spinning rate (6.5 kHz). The appearance of spinning side bands in the solid-state spectra is also indicative of a more anisotropic environment.

The observed resonances at δ *ca.* −600 are typical of a six-coordinate tin(IV) chloro species.[13] In the solid state the small chemical shift range observed of only 40 ppm between all the $SnCl_4$–dithioether complexes suggests that the tin centres are

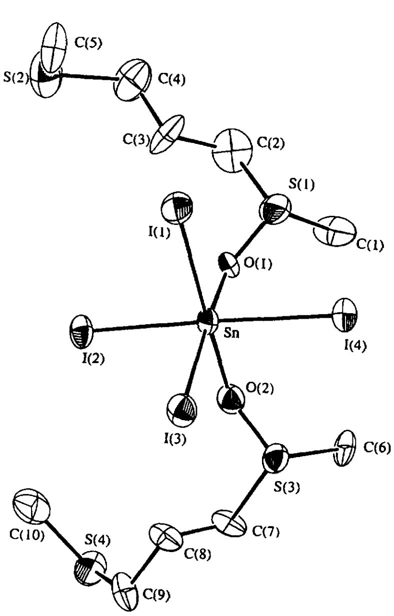

Fig. 7 View of the structure of *cis*-$[SnI_4\{MeS(O)(CH_2)_3SMe\}_2]$ with the numbering scheme adopted. Ellipsoids are shown at 40% probability

Table 7 Selected bond lengths (Å) and angles (°) for *cis*-$[SnI_4\{MeS(O)(CH_2)_3SMe\}_2]$

I(1)–Sn	2.788(2)	I(2)–Sn	2.762(2)
I(3)–Sn	2.780(2)	I(4)–Sn	2.802(2)
Sn–O(1)	2.21(2)	Sn–O(2)	2.18(1)
S(1)–O(1)	1.47(1)	S(1)–C(1)	1.78(2)
S(1)–C(2)	1.78(3)	S(2)–C(4)	1.79(3)
S(2)–C(5)	1.75(3)	S(3)–O(2)	1.52(1)
S(3)–C(6)	1.80(2)	S(3)–C(7)	1.79(2)
S(4)–C(9)	1.80(2)	S(4)–C(10)	1.76(3)
C(2)–C(3)	1.47(3)	C(3)–C(4)	1.53(3)
C(7)–C(8)	1.49(3)	C(8)–C(9)	1.55(3)
I(1)–Sn–I(2)	93.21(7)	I(1)–Sn–I(3)	97.13(7)
I(1)–Sn–I(4)	93.74(7)	I(1)–Sn–O(1)	92.0(4)
I(1)–Sn–O(2)	169.6(3)	I(2)–Sn–I(3)	93.64(6)
I(2)–Sn–I(4)	170.27(7)	I(2)–Sn–O(1)	84.1(4)
I(2)–Sn–O(2)	83.6(4)	I(3)–Sn–I(4)	92.25(7)
I(3)–Sn–O(1)	170.7(4)	I(3)–Sn–O(2)	92.9(3)
I(4)–Sn–O(1)	88.9(3)	I(4)–Sn–O(2)	88.4(4)
O(1)–Sn–O(2)	77.9(5)	O(1)–S(1)–C(1)	102(1)
O(1)–S(1)–C(2)	102(1)	C(1)–S(1)–C(2)	95(1)
C(4)–S(2)–C(5)	100(1)	O(2)–S(3)–C(6)	103.6(9)
O(2)–S(3)–C(7)	101.5(9)	C(6)–S(3)–C(7)	100.8(10)
C(9)–S(4)–C(10)	102(1)	Sn–O(1)–S(1)	122(1)
Sn–O(2)–S(3)	124.9(8)	S(1)–C(2)–C(3)	110(1)
S(2)–C(4)–C(3)	110(1)	S(3)–C(7)–C(8)	110(1)
S(4)–C(9)–C(8)	114(1)	C(2)–C(3)–C(4)	110(2)
C(7)–C(8)–C(9)	110(1)		

in very similar chemical environments. The chemical shift differences between the solid-state and solution NMR studies are probably attributable to solvent effects.[14] The chemical shift range of solution ^{119}Sn NMR spectroscopy is some 4000 ppm,[15] which suggests that significant differences might be expected in $\delta(^{119}Sn)$ on going from solution to the solid state. For example, studies on $[Sn(C_6H_{11})_3(OH)]$[14] have shown δ 11.6 in $CDCl_3$ solution and δ −217 in the solid state. Although the most dramatic differences are expected when a change in co-ordination occurs on going into solution, even slight geometrical changes can cause a shift of 50–100 ppm.[14]

The observation of a broad single line for the solid contrasts markedly to the low-temperature solution spectra which exhibit two sharp lines (separated by 1–2 ppm, attributable to the *meso*/DL isomers), and precludes identification of isomers in the solid state.

No resonance was observed in the solid state for any member of the $SnBr_4$–dithioether series despite long acquisition times and a variety of pulse/delay routines.

In an attempt to obtain crystals of $[SnI_4\{MeS(CH_2)_2SMe\}]$ suitable for an X-ray crystallographic study [this compound was identified *in situ* by solution $^{119}Sn\text{-}\{^1H\}$ NMR spectroscopy (δ −2645)], a $CHCl_3$ solution containing a 1:1 molar ratio of SnI_4 and $MeS(CH_2)_3SMe$ was allowed to evaporate slowly. This resulted in the formation of a red oil together with one or two red-orange crystals. A single-crystal X-ray analysis of one of these crystals revealed that during crystallisation oxidation of the ligand had occurred and the structure of the material isolated was in fact *cis*-$[SnI_4\{MeS(O)(CH_2)_3SMe\}_2]$ (Fig. 7, Table 7), involving a distorted-octahedral arrangement at Sn^{IV} *via* four iodide ligands and two O atoms from the sulfoxide functions of two mutually *cis* $MeS(O)(CH_2)_3SMe$ ligands, Sn–I 2.788(2), 2.762(2), 2.780(2), 2.802(2), Sn–O 2.21(2), 2.18(1) Å. Several examples of sulfoxide derivatives of tin(IV) halides have been reported,[16–18] however *cis*-$[SnI_4\{MeS(O)(CH_2)_3SMe\}_2]$ is unusual in that it was formed by oxidation of the dithioether $MeS(CH_2)_3SMe$ at one end only, giving an O-bound mixed sulfoxide–thioether ligand. This reaction presumably occurred through the presence of trace amounts of water in the reaction mixture. Attempts to prepare this compound in sufficient quantity to enable spectroscopic characterisation have not been successful. The Sn–I and Sn–O bond lengths are in accord with those in the literature, *e.g.* *cis*-$[SnCl_4(OSMe_2)_2]$ [Sn–Cl 2.369(3)–2.406(3), Sn–O 2.110(7), 2.110(8) Å],[16] *cis*-$[SnBr_4(OSMe_2)_2]$ [Sn–Br 2.531(3)–2.549(3), Sn–O 2.153(15), 2.205(15) Å][17] and *cis*-$[SnI_4(OSPh_2)_2]$ [Sn–I 2.773(1)–2.806(1), Sn–O 2.189(6), 2.249(6) Å].[18]

Conclusion

These results show that dithioether adducts of certain tin(IV) halides can be readily prepared, and the NMR spectroscopic data show that examples involving phenyl substituents are typically less stable than those involving methyl groups, with the complex stability decreasing with the SnX_4 acceptor: X = Cl > Br > I. This is supported by the trends observed in the Sn–X and Sn–S bond lengths derived from the X-ray crystallographic studies. Furthermore, ^1H and $^{119}Sn\text{-}\{^1H\}$ NMR spectroscopic studies show that the $[SnX_4(L\text{–}L)]$ systems are extremely labile in solution, with ligand-exchange and pyramidal-inversion processes both of low energy.

Experimental

Infrared spectra were measured as Nujol mulls using a Perkin-Elmer 983 spectrometer over the range 180–4000 cm^{-1}, variable-temperature ^1H NMR spectra using a Bruker AM360 spectrometer operating at 360 MHz and referenced to $SiMe_4$ (δ 0) and $^{119}Sn\text{-}\{^1H\}$ NMR spectra in 10 mm NMR tubes containing 10–15% deuteriated solvent using a Bruker AM360 spectrometer operating at 134.2 MHz and referenced to neat external $SnMe_4$ (^{119}Sn, δ 0). The complex $[Cr(acac)_3]$ (acac = acetylacetonate) was also added to the NMR solution as a relaxation agent prior to recording $^{119}Sn\text{-}\{^1H\}$ NMR spectra, to avoid signal diminution *via* the nuclear Overhauser effect resulting from the negative magnetogyric moment of the tin nucleus. Solid-state ^{119}Sn NMR spectra were obtained using a Bruker AM300 spectrometer fitted with a multinuclear solid-state probe at 111.9 MHz and 300 K. The material (400–500 mg) was packed into ZrO_2 or SiN rotors and data collected using a spinning speed of 4.5–6.5 kHz for best spectra. Typical spectral parameters were: contact time 6 μs, recycle time 2 s and number of transients 20 000. Spectra were rerun at lower speeds

Table 8 Crystallographic data

	[$SnCl_4\{MeS(CH_2)_2SMe\}$]	[$SnCl_4\{MeS(CH_2)_3SMe\}$]	[$SnCl_4\{o\text{-}C_6H_4(SMe)_2\}$]	[$SnCl_4\{PhS(CH_2)_3SPh\}$]	[$SnBr_4\{MeS(CH_2)_3SMe\}$]	[$SnI_4\{MeS(O)(CH_2)_3SMe\}_2$]
Formula	$C_4H_{10}Cl_4S_2Sn$	$C_5H_{12}Cl_4S_2Sn$	$C_8H_{10}Cl_4S_2Sn$	$C_{15}H_{16}Cl_4S_2Sn$	$C_5H_{12}Br_4S_2Sn$	$C_{10}H_{24}I_4O_2S_4Sn$
M	382.74	396.77	430.79	520.91	574.58	930.85
Colour, morphology	Colourless, block	Colourless, block	Colourless, column	Yellow, block	Colourless, block	Orange, column
Crystal dimensions/mm	0.30 × 0.25 × 0.10	0.40 × 0.20 × 0.20	0.50 × 0.20 × 0.10	0.40 × 0.30 × 0.15	0.30 × 0.30 × 0.20	0.20 × 0.20 × 0.05
Crystal system	Orthorhombic	Tetragonal	Triclinic	Monoclinic	Tetragonal	Triclinic
Space group	$Aba2$	$I\bar{4}2d$	$P\bar{1}$	Cc	$I\bar{4}2d$	$P\bar{1}$
a/Å	11.605(2)	10.107(2)	8.245(3)	7.763(2)	10.330(5)	10.545(6)
b/Å	8.918(3)	10.107	11.241(4)	13.893(3)	10.330	15.24(1)
c/Å	11.790(2)	24.726(3)	8.162(2)	17.611(2)	25.867(8)	8.284(5)
α/°			90.55(3)			95.42(5)
β/°			98.01(3)	93.75(2)		94.15(5)
γ/°			109.69(2)			108.69(5)
U/Å^3	1220.2(5)	2525.8(9)	703.9(4)	1895.2(6)	2760(2)	1247(1)
Z	4	8	2	4	8	2
F(000)	736	1536	416	1024	2112	852
D_c/g cm^{-3}	2.083	2.087	2.032	1.825	2.765	2.478
μ(Mo-Kα)/cm^{-1}	32.56	31.50	28.42	21.24	137.25	63.10
Transmission factors (maximum, minimum)	1.000, 0.721	1.000, 0.906	1.000, 0.686	1.000, 0.783	1.000, 0.578	1.000, 0.661
No. unique observed reflections	640	685	2479	1893	756	4405
R_{int} (based on F^2)	—	—	0.013	0.045	—	0.048
Unique reflections with [$I_o > 2.5\sigma(I_o)$]	531	583	2203	1450	509	2107
No. parameters	51	56	136	124	56	190
Goodness of fit	3.99	1.84	3.25	1.19	1.84	1.82
$R(F_o)$	0.031	0.023	0.039	0.023	0.047	0.051
$R'(F_o)$	0.035	0.032	0.042	0.031	0.056	0.054
Maximum, minimum residual peaks/e Å^{-3}	1.66, −0.86	0.70, −0.48	1.22, −2.42	0.44, −0.80	1.43, −1.15	1.75, −1.82

$R = \Sigma(|F_o|_i - |F_c|_i)/\Sigma|F_o|_i$, $R' = [\Sigma w_i(|F_o|_i - |F_c|_i)^2/\Sigma w_i|F_o|_i^{\,2}]^{\frac{1}{2}}$, goodness of fit $= [\Sigma(|F_o|_i - |F_c|_i)/\sigma_i]/(n - m) \approx 1$; n = no. of reflections measured, m = no. of independently refined parameters.

(2.5 kHz) to establish the central band position where spinning side bands were present. Spectra were referenced to $SnMe_4$ ($\delta = 0$) and a secondary reference of $SnCl_4$ (δ −150) was also employed. The magic angle was initially set using the ^{79}Br resonance of KBr. Microanalyses were obtained from the Imperial College microanalytical laboratory.

Tin(IV) fluoride was made by reaction of tin powder with fluorine at 300 °C (3 atm, *ca.* 3×10^5 Pa) in a Monel autoclave. Tin(IV) chloride and bromide were obtained from BDH and used as received. Tin(IV) iodide was made from the elements and recrystallised from $CHCl_3$. Thioethers were produced by previously reported methods.[19,20]

Syntheses

The complexes $[SnX_4(L\text{–}L)]$ [X = Cl or Br; L–L = $MeS(CH_2)_nSMe$, $PhS(CH_2)_nSPh$ (n = 2 or 3) or $o\text{-}C_6H_4(SMe)_2$] were all made by the same general method. The tin(IV) halides are moisture sensitive so all reactions were carried out in dry solvents under an atmosphere of dry nitrogen.

$[SnCl_4\{MeS(CH_2)_2SMe\}]$. Tin(IV) chloride (0.26 g, 1 mmol) was added to a solution of the thioether (0.12 g, 1 mmol) in chloroform (5 cm^3). The complex precipitated as a white powder which was filtered off, rinsed with chloroform and dried *in vacuo*. Yield 0.277 g, 73% (Found: C, 12.5; H, 2.4. Calc. for $C_4H_{10}Cl_4S_2Sn$: C, 12.6; H, 2.6%); $\tilde{\nu}$/cm^{-1} 326, 316, 307 and 301 (Sn–Cl).

$[SnCl_4\{MeS(CH_2)_3SMe\}]$. The same method yielded a yellow precipitate which was filtered off and dried *in vacuo*. Yield 0.33 g, 83% (Found: C, 15.3; H, 2.9. Calc. for $C_5H_{12}Cl_4S_2Sn$: C, 15.1; H, 3.1%); $\tilde{\nu}$/cm^{-1} 331, 321, 315 and 308 (Sn–Cl).

$[SnCl_4\{PhS(CH_2)_2SPh\}]$. The same method yielded a yellow precipitate which filtered off, rinsed with chloroform and dried *in vacuo*. Yield 0.39 g, 77% (Found: C, 33.0; H, 3.0. Calc. for $C_{14}H_{14}Cl_4S_2Sn$: C, 33.2; H, 2.8%); $\tilde{\nu}$/cm^{-1} 334, 327, 315 and 302 (Sn–Cl).

$[SnCl_4\{PhS(CH_2)_3SPh\}]$. The same method yielded a crop of orange crystals, which were filtered off, rinsed with chloroform and dried *in vacuo*. Yield 0.38 g, 73% (Found: C, 34.8; H, 3.4. Calc. for $C_{15}H_{16}Cl_4S_2Sn$: C, 34.6; H, 3.1%); $\tilde{\nu}$/cm^{-1} 339, 323, 316 and 309 (Sn–Cl).

$[SnCl_4\{o\text{-}C_6H_4(SMe)_2\}]$. The same method was used as for the first chloride species yielding white crystals which were filtered off, rinsed with chloroform and dried *in vacuo*. Yield 0.34 g, 79% (Found: C, 21.8; H, 2.2. Calc. for $C_8H_{10}Cl_4S_2Sn$: C, 22.3; H, 2.3%); $\tilde{\nu}$/cm^{-1} 332, 320, 311 and 304 (Sn–Cl).

$[SnBr_4\{MeS(CH_2)_2SMe\}]$. A saturated solution of tin(IV) bromide (2 mmol) in chloroform was added dropwise to a solution of 1,2-bis(methylsulfanyl)ethane (2,5-dithiahexane) in chloroform. A yellow precipitate formed immediately which was filtered off and dried *in vacuo* (Found: C, 8.8; H, 2.0. Calc. for $C_4H_{10}Br_4S_2Sn$: C, 8.5; H, 1.8%); $\tilde{\nu}$/cm^{-1} 238, 220, 216 and 209 (Sn–Br).

$[SnBr_4\{MeS(CH_2)_3SMe\}]$. The same method as for the previous bromide complex yielded a yellow precipitate which was filtered off and dried *in vacuo*. Yield 0.35 g, 61% (Found: C, 10.3; H, 1.9. Calc. for $C_5H_{12}Br_4S_2Sn$: C, 10.4; H, 2.1%); $\tilde{\nu}$/cm^{-1} 241, 220 and 206 (Sn–Br).

$[SnBr_4\{o\text{-}C_6H_4(SMe)_2\}]$. The same method was used again yielding a yellow precipitate which was filtered off and dried *in vacuo*. Yield 0.35 g, 58% (Found: C, 15.5; H, 1.3. Calc. for $C_8H_{10}Br_4S_2Sn$: C, 15.8; H, 1.6%); $\tilde{\nu}$/cm^{-1} 236, 224, 221 and 212 (Sn–Br).

X-Ray crystallography

Single crystals of $[SnCl_4\{MeS(CH_2)_2SMe\}]$, $[SnCl_4\{MeS(CH_2)_3SMe)\}]$, $[SnCl_4\{o\text{-}C_6H_4(SMe)_2\}]$, $[SnCl_4\{PhS(CH_2)_3SPh\}]$, $[SnBr_4\{MeS(CH_2)_3SMe\}]$ and *cis*-$[SnI_4\{MeS(O)(CH_2)_3SMe\}_2]$ were obtained by slow evaporation from a solution of the appropriate complex in either $CHCl_3$ or Me_2CO. For each compound the selected crystal was coated with mineral oil and mounted on a glass fibre. Data collection used a Rigaku AFC7S four-circle diffractometer equipped with an Oxford Cryostreams low-temperature attachment operating at 150 K, using graphite-monochromated Mo-Kα X-radiation (λ_{max} = 0.710 73 Å) and ω–2θ scans. The intensities of three standard reflections were monitored every 150. No significant crystal decay or movement was observed. As there were no identifiable faces the raw data were corrected for absorption using ψ scans. The weighting scheme $w^{-1} = \sigma^2(F)$ gave satisfactory agreement analyses in each case. Crystallographic data are presented in Table 8.

The structures of $[SnCl_4\{MeS(CH_2)_2SMe\}]$, $[SnCl_4\{MeS(CH_2)_3SMe\}]$, $[SnCl_4\{o\text{-}C_6H_4(SMe)_2\}]$ and *cis*-$[SnI_4\{MeS(O)(CH_2)_3SMe\}_2]$ were solved by direct methods,[21] while those of $[SnCl_4\{PhS(CH_2)_3SPh\}]$ and $[SnBr_4\{MeS(CH_2)_3SMe\}]$ were solved by heavy-atom methods.[22] All of the structures were then developed by iterative cycles of full-matrix least-squares refinement (on F) and Fourier-difference syntheses which located all non-H atoms in the asymmetric unit.[23] In each case all non-H atoms in the structures were refined anisotropically and H atoms were placed in fixed, calculated positions. For $[SnCl_4\{MeS(CH_2)_3SMe\}]$ and $[SnBr_4\{MeS(CH_2)_3SMe\}]$, both of which crystallise in the polar space group $I\bar{4}2d$, we attempted to establish the absolute configuration by inverting and translating the coordinates and re-refining to convergence. In both cases the enantiomorph chosen gave slightly lower R factors and estimated standard deviations associated with the atomic positions. The Hamilton R-factor ratio check also gave the same result.[24]

Atomic coordinates, thermal parameters and bond lengths and angles have been deposited at the Cambridge Crystallographic Data Centre (CCDC). See Instructions for Authors, *J. Chem. Soc., Dalton Trans.*, 1996, Issue 1. Any request to the CCDC for this material should quote the full literature citation and the reference number 186/243.

Acknowledgements

We thank the University of Southampton and the EPSRC for support, and the latter for a grant to purchase the diffractometer and the multinuclear MAS NMR probe.

References

1 I. R. Beattie, *Q. Rev. Chem. Soc.*, 1963, **17**, 382.
2 J.-M. Dumas and M. Gomel, *Bull. Chim. Soc. Fr.*, 1974, **10**, 1885.
3 N. C. Norman and N. L. Pickett, *Coord. Chem. Rev.*, 1995, **145**, 27.
4 S. J. Ruzicka and A. E. Merbach, *Inorg. Chim. Acta*, 1976, **20**, 221; 1977, **22**, 191; S. J. Ruzicka, C. M. P. Favez and A. E. Merbach, *Inorg. Chim. Acta*, 1977, **23**, 239.
5 C. T. G. Knight and A. E. Merbach, *Inorg. Chem.*, 1985, **24**, 576.
6 E. W. Abel, S. K. Bhargava, K. G. Orrell and V. Sik, *Inorg. Chim. Acta*, 1981, **49**, 25.
7 N. Bricklebank, S. M. Godfrey, C. A. McAuliffe and R. G. Pritchard, *J. Chem. Soc., Chem. Commun.*, 1994, 695.
8 G. R. Willey, A. Jarvis, J. Palin and W. Errington, *J. Chem. Soc., Dalton Trans.*, 1994, 255.
9 M. M. Olmstead, K. A. Williams and W. K. Musker, *J. Am. Chem. Soc.*, 1982, **104**, 5567.
10 E. W. Abel, S. K. Bhargava and K. G. Orrell, *Prog. Inorg. Chem.*, 1984, **33**, 1.

11 S. J. Blunden, D. Searle and P. J. Smith, *Inorg. Chim. Acta*, 1985, **98**, 185.
12 R. Colton, D. Dakternieks and C.-A. Harvey, *Inorg. Chim. Acta*, 1982, **61**, 1.
13 K. W. Zilm, G. A. Lawless, R. M. Merrill, J. M. Nillar and G. G. Webb, *J. Am. Chem. Soc.*, 1987, **109**, 7236.
14 R. K. Harris and A. Sebald, *Organometallics*, 1988, **7**, 388.
15 W. Petz, *Chem. Rev.*, 1986, **86**, 1019.
16 J. M. Kisenyi, G. R. Willey and M. G. B. Drew, *Acta Crystallogr., Sect. C*, 1985, **41**, 700.
17 M. Gregorkiewitz and D. Tudela, *Acta Crystallogr., Sect. C*, 1990, **46**, 210.
18 A. V. Jatsenko, S. V. Medvedev, K. A. Paseshnitchenko and L. A. Aslanov, *J. Organomet. Chem.*, 1985, **284**, 181.
19 F. R. Hartley, W. Levason, C. A. McAuliffe, S. G. Murray and H. E. Soutter, *Inorg. Chim. Acta*, 1979, **35**, 265.
20 T. Kemmitt and W. Levason, *Organometallics*, 1989, **8**, 1303.
21 SHELXS 86, program for crystal structure solution, G. M. Sheldrick, *Acta Crystallogr., Sect. A*, 1990, **46**, 467.
22 PATTY, The DIRDIF Program System, P. T. Beurskens, G. Admiraal, G. Beurskens, W. P. Bosman, S. Garcia-Granda, R. O. Gould, J. M. M. Smits and C. Smykalla. Technical Report of the Crystallography Laboratory, University of Nijmegen, 1992.
23 TEXSAN, Crystal Structure Analysis Package, Molecular Structure Corporation, Houston, TX, 1992.
24 W. C. Hamilton, *Acta Crystallogr.*, 1965, **18**, 502.

Received 10*th June* 1996; *Paper* 6/04072A